Harvard-Smithsonian Center for Astrophysics

Precision Astronomy Group

MEMORANDUM

Date: 13 April 1998 TM98-05
To: Distribution
From: R.D. Reasenberg
Subject: Spacecraft rotation, precession by means of gas jet impulses.

I. Introduction.

We consider a spinning spacecraft with the Z' axis (nominal spin axis) at an angle θ to the direction of the Z axis of an inertial coordinate system. For some purposes, it is useful to think of the Sun as being along the Z axis. In the spacecraft coordinate system, the nominal observing direction is along the X' axis. See Fig. 1 for the definition of the Euler angles that connect the two systems.

In Section II, we consider rotation dynamics: equations of motion and small angle perturbations due to an impulse of torque. We find that the nominal spin axis and the angular momentum vector are shifted (rotated) and an Eulerian nutation is excited by the impulse. Given these results, in Section III we investigate the rotational kinematics and corresponding consequences for the motion of a star image across the detector plane of a telescope rotating with the spacecraft. Similarly, in Section IV, the results of Section II are applied to the kinematics of precession and the overlap of observing bands. In Section V, we look at two special cases of spacecraft operations. In the first, a series of small torsional impulses precess the spacecraft. In the second, a pair of larger torsional impulses cause a change of spin axis orientation and, following that, the spacecraft is allowed to rotate without perturbation for an extended period. The further complications due to imperfect control of the torsional impulses (gas jet firings) are not considered, but would need to be factored into any analysis intended to select the method of precessing the spacecraft. Finally, in Section VI, the previously obtained results are applied to the FAME mission.

II. Rotation dynamics.

Following Goldstein[1] (p. 165), the Lagrangian for the spacecraft rotation is

[1] Goldstein, H., *Classical Mechanics*, Addison-Wesley, Reading Mass., 1959.

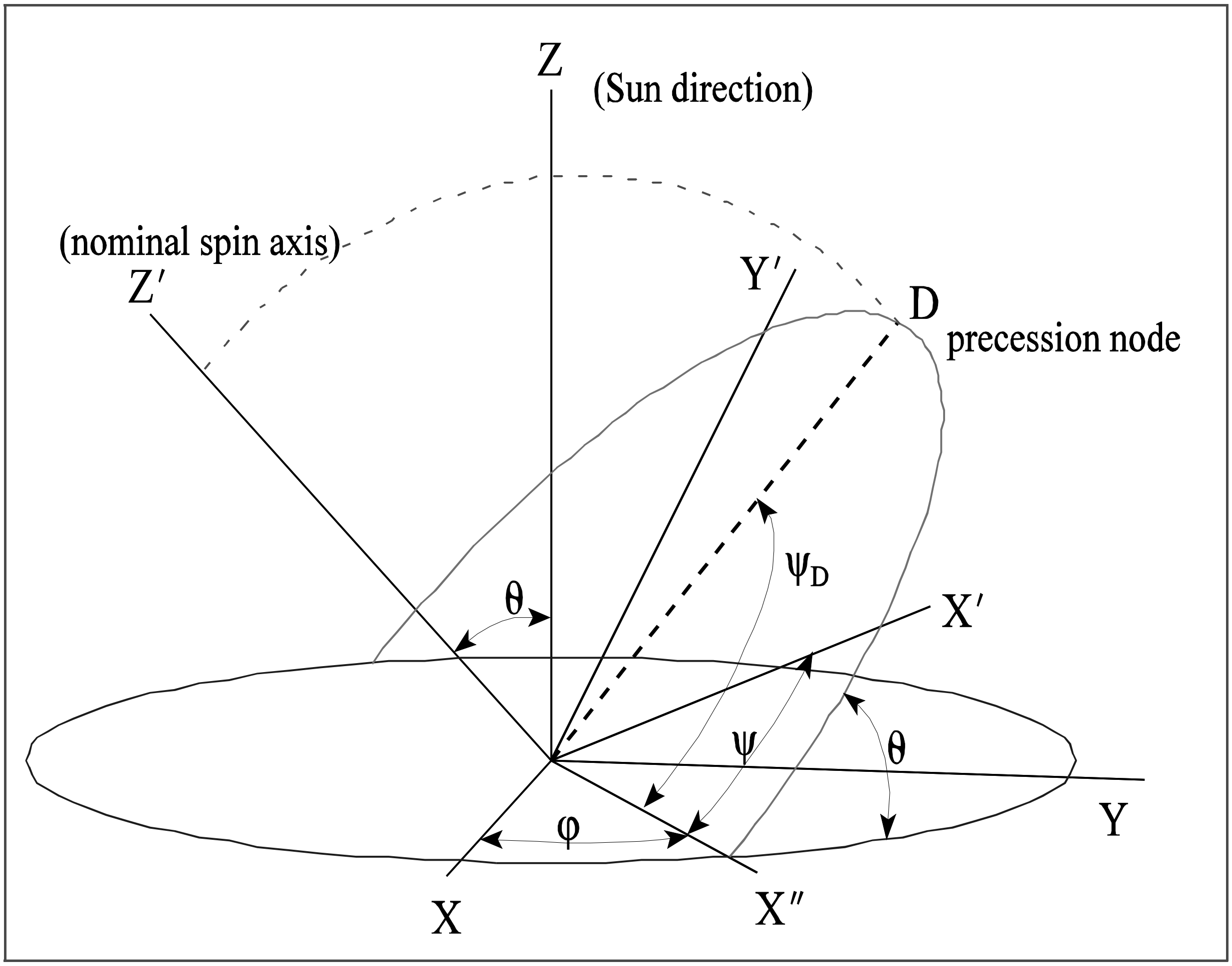

Figure 1. Rotations defining the spacecraft coordinate system (X′ Y′ Z′) in the (X Y Z) frame. The dashed arc is 90 degrees long and connects the Z′ axis and the precession node, D, which is shown as a dashed line in X′-Y′ plane. I passes through the Z axis when the precession is around Z. (Parenthetic labels refer to intended uses, which may not be a correct description in all cases.)

$$L = \frac{I_1}{2}(\dot{\theta}^2 + \dot{\varphi}^2 \sin^2\theta) + \frac{I_3}{2}(\dot{\psi} + \dot{\varphi}\cos\theta)^2 + N(t)\theta \qquad \textbf{(1)}$$

where N is a torque such that for N > 0, θ tends to increase, $I_1 = I_2$, and I_3 is around the nominal spin axis. In the chosen spacecraft coordinates, the moment of inertia tensor is diagonal. For the analysis below, the torque will be zero except during brief intervals. Lagrange's equation is applied for ψ and φ as in Goldstein's Eqs 5-46 and 5-47

$$I_3(\dot{\psi} + \dot{\varphi}\cos\theta) = I_3\omega_{z'} = I_1 a \qquad \textbf{(2)}$$

$$(I_1 \sin^2\theta + I_3 \cos^2\theta)\,\dot{\varphi} + I_3 \dot{\psi} \cos\theta = I_1 b \qquad \textbf{(3)}$$

where *a* and *b* are constants of the motion. The rotation period, $P = 2\pi/\omega_{z'}$, is also constant.[2] By combining Eqs 2 and 3, we obtain Goldstein's Eq 5-50

$$\dot{\varphi} = \frac{b - a\cos\theta}{\sin^2\theta} \qquad \textbf{(4)}$$

Next, Lagrange's equation is applied for θ to yield

$$I_1 \dot{\varphi}^2 \sin\theta\cos\theta - I_1 a \dot{\varphi} \sin\theta + N = I_1 \ddot{\theta} \qquad \textbf{(5)}$$

Initially (i.e., at t = 0), $\dot{\varphi}$, $\dot{\theta}$, and N are all zero, $\theta = \theta_0$, and $\varphi = \varphi_0$. Given these initial conditions, one finds from Eq 4 that $b = a\cos\theta_0$. From Eq 5, $\ddot{\theta}$ must also be zero at t = 0.

Consider a kick, an impulsive torque caused by a thruster firing.[3] Initially the spacecraft is spinning around the Z′ axis, and is neither precessing nor nutating. The impulse is characterized by

$$N(t) = \begin{cases} \dfrac{M_0}{\varepsilon}, & 0 < t < \varepsilon \\ 0 \;\;, & \text{all other} \end{cases} \qquad \textbf{(6)}$$

where $M_0 \equiv N_n \tau_n$ is an impulse of torque and thus the moment of an impulse of force, and N_n and

---

[2] The period is constant because there is no component of torque in the Z′ direction. In a more complete analysis of the spacecraft, we would consider smaller effects such as a mispointing of the gas jets, which would cause the spin rate to change each time the spacecraft received an impulse, or a spacial variations in the reflectivity of the shield, which would give rise to a spin rate that would vary with the rotation phase with respect to the Sun direction.

[3] In a more complete analysis, the thruster profile would be considered. For present purposes, it is sufficient to treat the thruster as producing an impulse of force.

τ_n are a nominal torque and its duration, respectively. M_0 is along the X″ axis (Fig. 1), and thus has no component along the spin axis. Then $M_0 = \hat{Z}' \times J_0$, where J_0 is the impulse of force that, acting on a unit arm along the spin axis, produces the required impulse of torque. (J_0 is in a direction that pushes the spin axis away from the Z axis.) During the short interval $0 < t < \varepsilon$ (where ε << P), the quantities θ, φ, and $\dot{\varphi}$ will not change significantly. (This is the impulsive approximation.) Thus, as a result of the thruster firing,

$$\Delta\dot{\theta} = \int_0^{\varepsilon} \frac{M_0}{I_1 \varepsilon} dt = \frac{M_0}{I_1} \tag{7}$$

which we treat in the limit as $\varepsilon \rightarrow 0$.

We next investigate the small-amplitude variation of θ and φ starting at $t = \varepsilon$, with the conditions following the kick. If we neglect second-order terms, Eq 5 takes the form

$$\ddot{\theta} = -a\dot{\varphi}\sin\theta \tag{8}$$

Eqs 4 and 8 together suggest the following approximation

$$\begin{aligned} \theta &= \theta_0 + \theta_c + \delta \\ \delta &= \theta_2 \sin(\Omega t + \xi) \end{aligned} \tag{9}$$

where θ_c is the constant of integration, determined below to be zero. By applying the first of these to Eqs 4 and 8 , we obtain

$$\ddot{\delta} = -a^2 \delta \tag{10}$$

where use has been made of $b = a\cos\theta_0$. By applying the second of Eqs 9, we find $\Omega = a$. Since at $t = \varepsilon$, $\ddot{\theta} = 0$, it must also be that $\xi = 0$. By incorporating Eq 7, we obtain

$$\theta = \theta_0 + \frac{M_0}{I_1 a} \sin(at) \tag{11}$$

where the constant of integration is set by the requirement that $\theta \rightarrow \theta_0$ as $t \rightarrow 0$.

We next apply Eq 11 to Eq 4 and use $b = a\cos\theta_0$ to obtain

$$\dot{\varphi} = \frac{M_0}{I_1 \sin\theta_0} \sin(at) \tag{12}$$

which can be integrated to yield

$$\varphi = \varphi_0 + \frac{M_0}{I_1 a \sin\theta_0} (1 - \cos(at)) \tag{13}$$

In Eq 13, the constant of integration was set by the requirement that $\varphi \to \varphi_0$ as $t \to 0$. Thus, following the kick, the Z′ axis moves in a circle of radius M_0/aI_1 that passes through the initial position and is centered on a point Q displaced in the φ direction by a distance M_0/I_1a. (In describing a radius and a distance, one can refer to central angles of the spherical coordinate system or to distances, which are properly described using a local Cartesian coordinate system such as the one discussed in connection with Fig. 2. The extra factor of $1/\sin\theta_0$ in Eq 13 is an artifact of the spherical coordinate system.) The point Q represents the location of the angular momentum vector of the spacecraft following the kick. The angular momentum had coincided with the Z′ axis before the kick.

III. Rotational kinematics and the motion of the view direction.

The motion of the X′ axis around the Z′ direction is the nominal spin, $\omega_{z'} = \dot{\psi} + \dot{\varphi}\cos\theta$. However, there is also a motion of the X′ axis around the Y′ direction, which causes the star images to move diagonally with respect to the nominal track in the camera. This is described by

$$\omega_{y'} = \dot{\varphi} \sin\theta \cos\psi - \dot{\theta} \sin\psi \tag{14}$$

where $\psi = \psi_0 + \dot{\psi} t$. By using Eqs 11 and 12, we obtain

$$\omega_{y'} = \frac{M_0}{I_1} \sin\left(\omega_{z'} \frac{I_3 - I_1}{I_1} t + \zeta \right) \tag{15}$$

where ζ is an initial phase.[4] There is a corresponding cosine term for $\omega_{x'}$. The spin vector moves around the Z' axis in the rotating spacecraft frame. For $I_3 > I_1$, the spin vector is on the far side of Q from Z'. (For the rotation of the Earth, the corresponding motion is called the Chandler wobble.)

The angle (with respect to the X'-Y' plane) at which the spacecraft rotation causes the stars to move across the field of view is $\beta \approx \tan\beta = \omega_{y'} / \omega_{z'}$. Equations 2 and 15 show that this angle varies over the range $\pm\tilde{\beta}$, and that $\tilde{\beta} = M_0 I_3 / I_1^2 a = M_0 / I_1 \omega_{z'}$. This path deviation sets one practical limit to the acceptable rate of spacecraft precession because of the effective lateral smearing of the target stars on the detector.

IV. Kinematics of precession and the overlap of observation bands.

Smooth precession may be described by a constant rate of change of φ, see Fig. 1. This rate may be usefully projected along two axes, Z' $(\dot{\varphi}\cos\theta)$ and the line of nodes, D $(\dot{\varphi}\sin\theta)$. The former is a component of the spin rate, as seen in Eq 2. The latter causes successive rotations of the spacecraft to trace out shifted observing bands. If the change of φ from one rotation to the next is $\Delta\varphi$, then the separation of band centers is about $\Delta\varphi \sin(\theta) \sin(\psi-\psi_D)$. Thus, for an observing band of width W, the maximum change in φ that will not leave gaps in the sky coverage is $W/\sin(\theta)$.

One of the early SAO-developed optical designs for FAME had W = 0.75 deg and θ = 45 deg. For this case, the maximum gap-free precession rate is about 1 deg per revolution. At 12 revolutions per day (the nominal associated with that design), a precession cycle would take 30 days. A longer precession cycle would permit overlap at the part of the observing band 90 deg from the precession node. Thus, the nominal precession rate of once per 60 days yields a 50% overlap at a point 90 deg from D, and an 84% overlap of area between successive observation bands.

The present nominal optical design has W = 2.2 deg and θ = 45 deg. The precession rate is limited by lateral smear of the star (bound on $\tilde{\beta}$) to about $\Delta\varphi$ = 0.5 deg per spacecraft rotation. This leads to multi-revolution overlap, even at 90 deg from the line of nodes.

---

[4] The amplitude of this periodic component of rotation is simply the torsional impulse divided by the corresponding principal moment of inertia: $\omega_{y'} = M_0/I_1$. Just after the kick, we find that the angular momentum vector has moved to a new position (in inertial space), and the Z' axis has been given the motion associated with $\omega_{y'}$.

V. Spacecraft operations.

In the geometry used above, the kick is such as to increase the angle between the Sun direction and the spacecraft Z' axis. Consider a torsional impulse $M_a = \hat{Z}' \times J_a$, where J_a acts at an angle ν to the desired average direction of precession, as shown in Fig. 2. (Up to now, we had used a kick geometry characterized by $\nu = \pi/2$.) After a nutation by 2ν, we apply a kick $M_b = \hat{Z}' \times J_b$ where J_b acts normal to the desired average direction of precession; the latter starts a new nutation, which has the same shape as the old nutation, but is displaced in the φ direction. Then,

$$\begin{aligned} \Delta T &= 2\frac{\nu}{a} \\ M_b &= 2 M_a \sin\nu \\ \Delta\varphi &= \frac{2 M_a \sin\nu}{I_1 a \sin\theta_0} \end{aligned} \qquad \textbf{(16)}$$

where ΔT is the interval between kicks. From these, we obtain the ratios

$$\begin{aligned} \frac{M_b}{\Delta\varphi} &= I_1 a \sin\theta_0 \\ \frac{\Delta\varphi}{\Delta T} &= \frac{M_a}{I_1 \sin\theta_0}\,\frac{\sin\nu}{\nu} \end{aligned} \qquad \textbf{(17)}$$

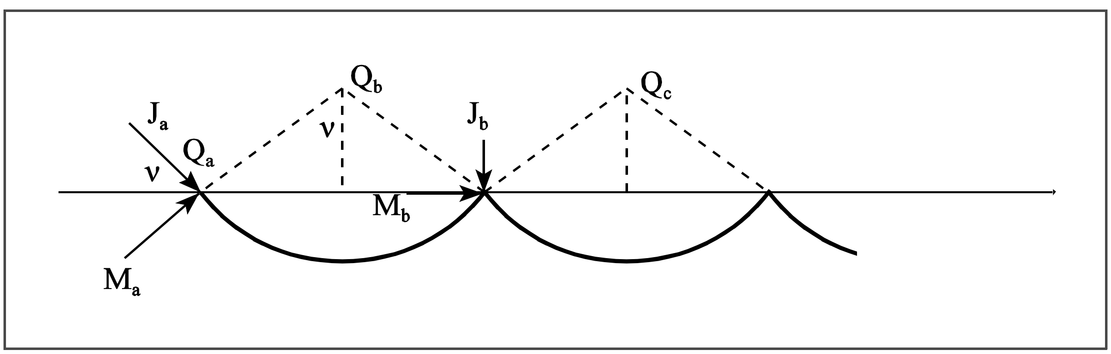

Figure 2. Motion of the spacecraft Z' axis (series of arcs) as a result of a series of kicks (torsional impulses, M, and the corresponding force impulses, J). The long straight line is the nominal precession trajectory, which in Fig. 1 would be a “small circle” with center at Z and passing through Z'. [Figure 2 uses a local Cartesian coordinate system: abscissa, $\varphi/\sin\theta_0$; ordinate, θ.]

where the former is the impulsive torque per change of φ, and the latter is the average precession rate. Since $\tilde{\beta}$, the range of swing of β, depends on M_a and not on ν, for a fixed average precession rate, $\tilde{\beta} \propto \nu/\sin\nu$. Letting $\nu = \pi/2$ increases $\tilde{\beta}$ by a factor of $\pi/2 \approx 1.57$ over the value for small ν. (I see no reason for operating with ν greater than about $\pi/2$.) Note that using torque produced by radiation pressure to precess the spacecraft yields the same $\tilde{\beta}$ as the small-ν case (i.e., with repeated small kicks). However, the radiation-pressure torque is smooth, and thus does not break the rotation into segments requiring additional parameters to be estimated.

We next consider an alternative scheme in which there are a pair of large kicks M_ℓ in nearly opposite directions, separated by a short interval $\Delta T = \kappa P << P$, where P is the period of rotation. The spacecraft is precessed during the short interval, during which β may be too large for taking data. Then, for a longer interval (e.g., P - ΔT), the spacecraft spins (about the Z′ axis) with $\beta = 0$. The ratio of total impulsive torque to corresponding change of φ is

$$\frac{2\,M_\ell}{\Delta\varphi} = \frac{I_1\,a\,\sin\theta_0}{\sin\nu} \qquad \textbf{(18)}$$

where $\nu = \pi\kappa I_3/I_1$. For small κ, $\sin\nu \approx \nu$ and

$$\frac{2\,M_\ell}{\Delta\varphi} \approx I_1\,a\,\sin\theta_0\,\frac{I_1}{\pi\kappa I_3} \qquad \textbf{(19)}$$

Thus for example, for $\kappa = 0.1$ (and $I_3 = 1.25\,I_1$), the required kick is increased a factor of 2.5 and the observing time is reduced 10% compared to the case of small ν and repeated (M_b) kicks. These disadvantages must be seen in comparison to the gain in coherence discussed in TM98-04. Table 1 of that memo (which contains results from TM98-02) shows that the coherence of the spiral reduction is increased 4.4 fold by changing from an average of six spans per rotation to an average of one span per rotation: $\sigma(\Delta\varphi) / \sigma_0$ is reduced from 2.9 (unacceptable) to 0.66 (barely acceptable). By having only one span in the six-rotation spiral, $\sigma(\Delta\varphi) / \sigma_0$ became 0.26, and a further two-fold reduction was shown by increasing the spiral and span lengths by a factor of four. This level for $\sigma(\Delta\varphi) / \sigma_0$ seems likely not to degrade the mission accuracy.

We next consider a strategic approach to the two-kick scheme described above. For this purpose, we consider the spacecraft to have two observing directions, equally spaced (in opposite directions) by a modest angle (less than 1 radian) from the X′ axis. I offer the following hypothesis, which would need to be tested by appropriate simulations:

> It would be advantageous to tailor the timing of the kicks so that at their mean epoch the X′ axis is centered on one of the areas of observational overlap between successive rotations. This should facilitate tying together in the data analysis both (1) the two successive spans and (2) the corresponding points of the rotation of the two observing

directions (i.e., to yield closure) for each span. This overlap is greatest near the precession node, shown in Fig. 1 as a dashed line in the X'-Y' plane, and at an angle ψ_D from the X'' axis, where ψ_D = 90 deg when the precession is around the Z axis. Thus, the pair of big kicks are timed so that at their respective epochs the values of ψ-ψ_D are of equal magnitude and opposite sign. This approach disrupts the observations in the region that locally has the maximum overlap and therefore degrades the observations of the stars that are locally observed most redundantly.

Following this hypothesis, one would expect to see the gas jets firing at the same rotation phase (ψ) during each rotation. However, there is an alternative approach that I believe would be advantageous. For this approach, the complete cycle requires three rotations during which there are two sets of (two) gas-jet firings. The cycle starts with a pair of gas-jet firings in accord with the above hypothesis. After one and a half rotations (from the initial firing) there is another pair of gas-jet firings. These occur at 180 deg (in ψ) from the first set. Finally, the spacecraft completes its three rotations, returning to the rotation phase at which the first gas-jet firing occurred, and the cycle repeats.

With this approach, the disruptions of the observations are divided between the northern and southern hemispheres, and the disrupted regions are re-observed during the next two rotations. Because of this arrangement, the interval between the two jet firings can be extended, thus decreasing the gas usage. The added burden of gas use associated with this approach is determined by combining Eqs 17, 18 and using $\nu = \pi\kappa I_3/I_1$

$$\frac{2M_\ell}{M_b} = \frac{1}{\sin(\pi\kappa I_3/I_1)} \qquad \textbf{(20)}$$

where $2M_\ell/M_b$ is the ratio of required gas use rates assuming identical mean precession rates and the availability of jets mounted in the desired direction. For example, if I_3/I_1 = 5/4 and the gas-jet firings are separated by 90 deg (κ = 0.25), then the gas use is increased by a factor of 1.20 as compared to a series of firings as described above. For a separation of 144 deg (κ = 0.4), there is no increase in gas use.

For a fixed set of gas jets, the torque would be produced by firing two of the jets to produce the required vector sum. This approach yields a trade between the number of jets and the efficiency of the process. A plausible number of jets, ignoring the question of redundancy, is five. In an alternative approach, a smaller number of jets (say three) are mounted on a turret that is able to rotate by a modest angle (say ± 90 deg), so as to permit fine control of the direction of the thrust. This use of turret-mounted jets adds the cost and complexity of a mechanism, and is thus unlikely to be justified.

VI. Discussion.

Here we consider the requirements for spacecraft rotation imposed by the FAME mission. It is intended that FAME will use a version of the HIPPARCOS observing pattern in which the spacecraft spins to allow the observation of stars in a band at right angles to the spin axis; the spin axis slowly precesses around the Sun direction. That precession could be either continuous or in discrete steps. Independent of the mechanism used to produce the precession, while it is taking place, it will cause the targets to move along the detector at an angle that will vary with the rotation phase of the spacecraft.

Continuous precession (driven by continuously applied torque) has the advantage that the observations are not segmented by attitude-control events into (short) spans. Such segmentation would adversely affect the information return from the mission. There are several possible ways of producing continuous torque. Magnetic torque bars can operate only at low altitude, and cannot operate in all directions. Rotating-wheel systems are believed to produce too much vibration to be applicable to an astrometric mission. (This assumption should be tested at some time before the design is frozen.) Adjustable, ultra-low thrust, gas jets are not presently available, although an interesting system has been described using heated Palladium and diffusing H_2.[5] Solar radiation pressure acting on a large shield can produce the desired torque. However, at low rotation rates (e.g., two hours per revolution) with a large shield, the shape of the shield would need to be adjusted precisely to reduce the torque (10 to 100 fold) to an acceptable level. For higher spin rates, the shape adjustment is not so critical.

If impulsive gas jets are to be used to affect the precession, then there are two viable scenarios. In the first, there are a series of attitude-control events, say five or more spaced more or less evenly around one rotation of the spacecraft. In the second, there are two attitude-control events per spacecraft rotation (or per a larger multiple of ½ rotation), but these are relatively large, and likely preclude observing between the events. The latter approach uses significantly more ACS fuel than the former, but permits most of the observing to take place from a non-precessing spacecraft. Assuming a reasonable ratio of principal moments of inertia, it would not be possible to have only a single attitude-control event per rotation.

A further complication of the use of gas jets is that the magnitude of each firing has a variance, and the direction of action of each jet will deviate from that intended. The latter would result in the jets causing a change in the spin rate. If severe, this would cause a loss of precise data until the spin rate could be determined from crudely-taken data, and the CCD clock rate adjusted accordingly. This would be an undesirable mode, but the corresponding loss of information may need to be quantified before the trade is made among methods of precessing the spacecraft.

---

[5] Gilmore, in an invited paper on GAIA at SPIE Conference 3350 (Kona, 3/98), said that they were planning to use ion engines to precess the spacecraft.

VII. Acknowledgments.

I thank J.F. Chandler and J.D. Phillips and especially M. Mook for reviewing this memorandum in draft form.

VIII. Distribution.

SAO:	USNO & NRL via PKS:	Other:
R.W. Babcock	M.E. Germain	M.E. Ash (CSDL)
J.F. Chandler	K.J. Johnston	
J.D. Phillips	M. Mook	
R.D. Reasenberg	M.A. Murison	
I.I. Shapiro	P.K. Seidelmann	
	S.E. Urban	